Experimental study of water evaporation from nanoporous cylinder surface in natural convective airflow

S. Hara
Department of Mechanical Engineering, Toyo University, Japan

Abstract

Unglazed porous cylinders were used to study experimentally the evaporation features of water from the cylinder surfaces in natural convective airflows. Seto semi-porcelain clay No.6 was employed to make the unglazed porous cylinders. The firing temperature was changed from 773 to 1523 K to regulate the pore size of the porous. The diameter was from 80 to 85 mm, the thickness 7 mm, and the span 290 mm. The experiment was made at constant air temperature and the relative humidity. The air temperature ranged from 284 to 297 K and the relative humidity from 40 to 72%. The firing temperature had little effects on the evaporation characteristics. The evaporation rates were always 2.5 to 4 times as high as those of non-porous cylinders. The Grashof number, which shows macroscopic natural convection, did not have any appreciable effects on the evaporation. The evaporation rates were affected by the ambient temperature and relative humidity. Therefore, the following two conclusions were acquired: the evaporation on the nanoporous walls should be largely taken into account with the interaction between water and surface molecules which determines the evaporation energy of molecules, and the nanoporous does not consist of the pores among particles of the semi-porcelain, but of the nanoscale pores of a particle.
Keywords: water evaporation, natural convection, nanoporous surface, unglazed semi-porcelain cylinder, molecular interaction, firing temperature, nanoscale pore, experiments, air temperature, relative humidity.

WIT Transactions on Engineering Sciences, Vol 53, © 2006 WIT Press
www.witpress.com, ISSN 1743-3533 (on-line)
doi:10.2495/HT060451

1 Introduction

Water evaporation phenomenon has been observed for water contained in an unglazed semi-porcelain cylinder. The mechanism of the evaporation from the nanoporous surface is unknown. If the porous passage is large enough for water molecules moving to surface, the evaporation on the porous surface goes on in the same manner as on the surface of water film, showing the same evaporation rate of the later. If the passage is resistive for the water molecules, the molecular interaction must be appreciable between the passage and the passer-by molecules. The evaporation latent heat is macroscopically defined as the energy difference between gaseous and liquid states of the molecular assembles at the same temperature and pressure. This means that it is the energy required for molecules to leave away the liquid-state cluster of the same homogeneous molecules. If the third molecules are related to the process of evaporation as in the solid-state cluster, the evaporating energy of the molecules must be different from that of the homogeneous molecules as shown in references [1 ~ 6]. Whether the change is positive or negative depends on the third-body interaction with the evaporating molecules. Concerning the water evaporation on the nanoporous surface of the unglazed pottery cylinder in forced convective airflow as shown in the references [7, 8], the evaporation rates were 2.5 times as high as those of non-porous cylinders at first. However, these evaporation rates decreased to the equilibrium value of 1.5 after 30 minutes. This is why the surface dry causes the water supply rate from the inside of the cylinder to be less than the evaporation rate from the surface of the cylinder. Therefore, the water evaporation on the surface of the nanoporous cylinders was not able to be detailedly analyzed. But in the natural convective airflow the cylinder surface does not get dry because the evaporation rate is low, and the evaporation rate remains steady as the time passes. It was, therefore, experimentally investigated how the water evaporation will be affected by the nanoscale pore size of the cylinder surface. The experiment was carried out in natural convective evaporation on the ground-based nanoporous cylinder with water inside.

2 Experimental apparatus and procedure

Figure 1 shows the experiment apparatus used. The nanoporous cylinder of 80 mm in diameter and 290 mm in length is surrounded by 700×700 mm cross-sectional area and 1000 mm high walls for getting stable natural convection. The walls are 700 mm away from the ground. The cylinder is located on the supporting cylinder of 80 mm in diameter and 1000 mm in height from the ground. Distilled water was absorbed up into the hollow cylinder of 7 mm in thickness from the storage tank, where the water surface level is 100 mm below the underneath end of the cylinder. Seto semi-porcelain clay No.6 is used to make the cylinder and the firing temperature was changed between 773 and 1523 K. The firing temperature causes the size of porous pores to change between 5 nm and 100 nm. The experiment was carried out under the stable

conditions of the room temperature and relative humidity and with possible reduction of global natural convections in the room.

The experiment started on the wetted surface of the cylinder. The evaporation rate was measured by the water flow supplied into the porous cylinder with a flow meter of Peltier element. The air temperature was measured with Pt 100 thermometer. The relative humidity was measured with HUMICAP of Vaisala (thin-film polymer sensor). The experimental air temperature T was 284 to 297 K and the relative humidity RH 40 to 72%.

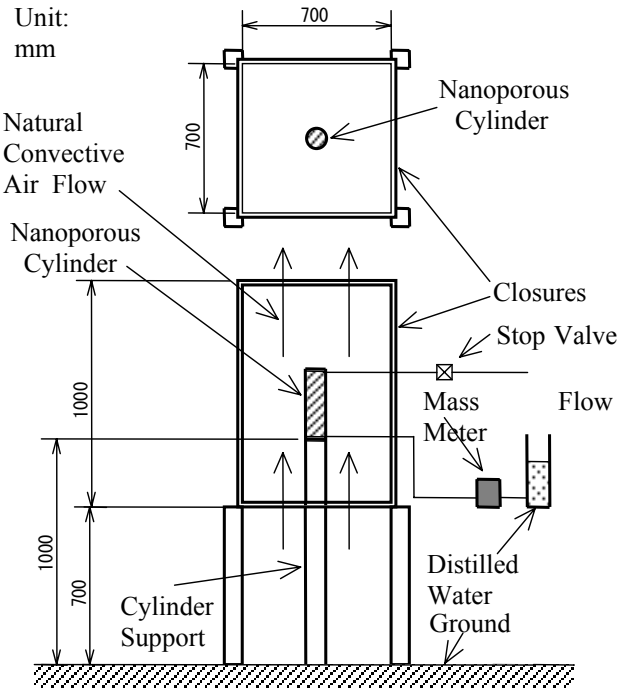

Figure 1: Experimental apparatus.

3 Experimental results

The experimental results obtained are summed up using two non-dimensional parameters, Sh; the Sherwood number for evaporation rate and Gr; the Grashof number for natural convection. The Sherwood number shows the evaporation rate, compared with the molecular diffusion rate under the same molecular-density conditions at the boundary. The evaporation rate can be expressed as

$$h_D \left(\rho_\infty - \rho_w\right) S, \tag{1}$$

and the molecular diffusion rate is given by

$$D \frac{\rho_\infty - \rho_w}{d} S, \tag{2}$$

where ρ_w and ρ_∞ are the water concentrations or air densities at the cylinder-wall surface and its infinity, h_D the total mass transfer rate at the cylinder surface, D the molecular diffusion coefficient, d the cylinder diameter, and S the total surface area causing the evaporation. Then the Sherwood number is shown as

$$\mathrm{Sh}_d \equiv \frac{h_D \cdot d}{D} \ . \tag{3}$$

The Grashof number is an inertial force compared with the viscous force like as the Reynolds number, although the inertial force without any forced flows is given by the natural convection force as

$$\rho_\infty \frac{u^2}{d} = g\ (\rho_\infty - \rho_w)\ , \tag{4}$$

and the viscous force is given by

$$\rho_\infty \cdot \nu \frac{u}{d^2}\ , \tag{5}$$

where u is the characteristic velocity and ν the kinematic viscosity. These give the non-dimensional number, Gr_d ; Grashof number as

$$\mathrm{Gr}_d \equiv \left\{ \left(\rho_\infty \frac{u^2}{d} \right) \Big/ \left(\rho_\infty \cdot \nu \frac{u}{d^2} \right) \right\}^2 = \frac{u^2 \cdot d^2}{\nu^2} = g \frac{\rho_\infty - \rho_w}{\rho_\infty} \frac{d^3}{\nu^2}\ , \tag{6}$$

The heat transfer handbook [9] shows the Nusselt number for the cylindrical surface as

$$\frac{\left(\mathrm{Nu}_l^*\right)_c}{\left(\mathrm{Nu}_l^*\right)_p} = 1 + 0.428 \left\{ \frac{2l/d}{\left(\mathrm{Nu}_l^*\right)_p} \right\}^{5/6}\ , \tag{7}$$

where $\left(\mathrm{Nu}_l\right)_c$ is the Nusselt number for the circular cylinder based on the cylinder length l and $\left(\mathrm{Nu}_l\right)_p$ is the Nusselt number for the flat plate and with the plate length l. Since the latter is given as

$$\left(\mathrm{Nu}_l^*\right)_p = 0.515\,\mathrm{Ra}_l^{1/4}\ , \tag{8}$$

$$\left(\mathrm{Nu}_l\right)_c = 0.515\ \mathrm{Ra}_l^{1/4} + 0.683 \left(l/d\right)^{5/6} \mathrm{Ra}_l^{1/24}\ , \tag{9}$$

or eqn. (7) gives

$$\left(\mathrm{Nu}_d^*\right)_c = 0.515\ \left(\mathrm{Ra}_d \cdot d/l\right)^{1/4} + 0.683\ \left(\mathrm{Ra}_d \cdot d/l\right)^{1/24}\ , \tag{10}$$

where $\left(\mathrm{Nu}_d\right)_c$ and Ra_d are the Nusselt number and Rayleigh number based on the cylinder diameter d. Since Ra_d is given as

$$\mathrm{Ra}_d = \mathrm{Gr}_d \cdot \mathrm{Pr}\ , \tag{11}$$

$$\left(\mathrm{Nu}_d^*\right)_c = 0.515\ \left(\mathrm{Gr}_d \cdot \mathrm{Pr} \cdot d/l\right)^{1/4} + 0.683\ \left(\mathrm{Gr}_d \cdot \mathrm{Pr} \cdot d/l\right)^{1/24}\ . \tag{12}$$

Substituting Nu with Sh, and Pr with Sc to eqn. (12) by the analogy between heat and mass transfer, then the Sherwood number for the non-porous cylinder fully wetted by water is given by

$$\left(\mathrm{Sh}_d^*\right)_c = 0.515\left(\mathrm{Gr}_d \cdot \mathrm{Sc} \cdot d/l\right)^{1/4} + 0.683\left(\mathrm{Gr}_d \cdot \mathrm{Sc} \cdot d/l\right)^{1/24}, \qquad (13)$$

where Sc is the Schmidt number. It is the purpose of the present experiment how different evaporation rates Sh will be resulted in the water evaporation from the nanoporous surfaces, under the same natural convective conditions, Gr. The evaporation rates resulted are all given in the term of the ratio compared with the Sherwood number for the fully wetted cylindrical surfaces at the same Grashof number, $\mathrm{Sh}_d / \mathrm{Sh}_d^*$ vs. Gr_d.

3.1 Effects of the firing temperature on the cylinder porous

3.1.1 Effects of the firing temperature on the cylinder diameter

Figure 2 shows the effect of the firing temperature on the cylinder diameter. The shape, size and porosity distribution will be affected by the firing temperature to make the unglazed porous cylinder from the clay. The diameter of the semi-porcelain cylinder remained stable by 1273 K, and then the diameter decreased rapidly as the firing temperature increase.

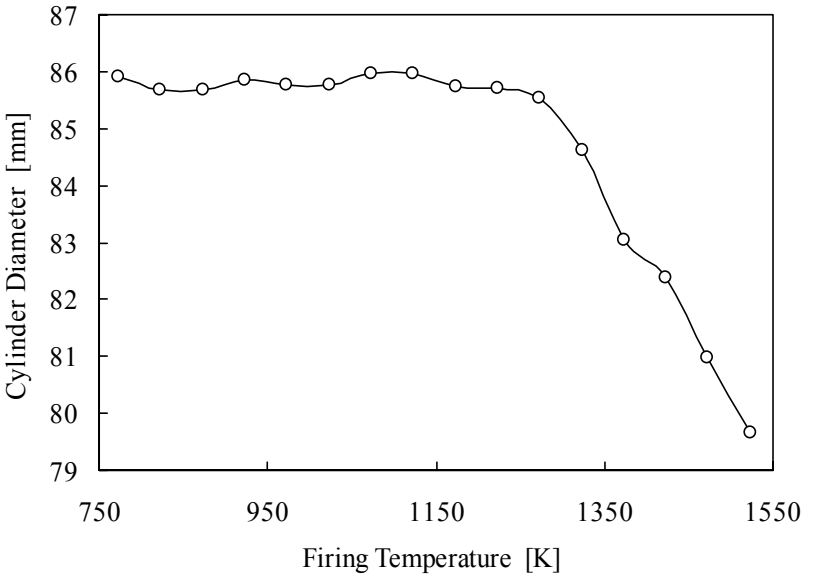

Figure 2: Effects of the firing temperature on the cylinder diameter.

3.1.2 Effects of the firing temperature on the water leakage mass rate

Figure 3 shows the effect of the firing temperature on the water leakage mass rate at the loaded pressure of 500 mm Aq. The water leakage mass rate raised as the firing temperature increased by 1373 K, and then the water leakage mass rate fell rapidly as the temperature increased. At 1523 K, there was no leakage.

Specifically, the size of the pore among the semi-porcelain particles came to be smaller as the temperature increased by 1373 K, then the size of the pore rapidly decreased, and at the temperature of 1523 K there was no leakage. This shows that the pore size among the semi-porcelain particles changed due to the firing temperature.

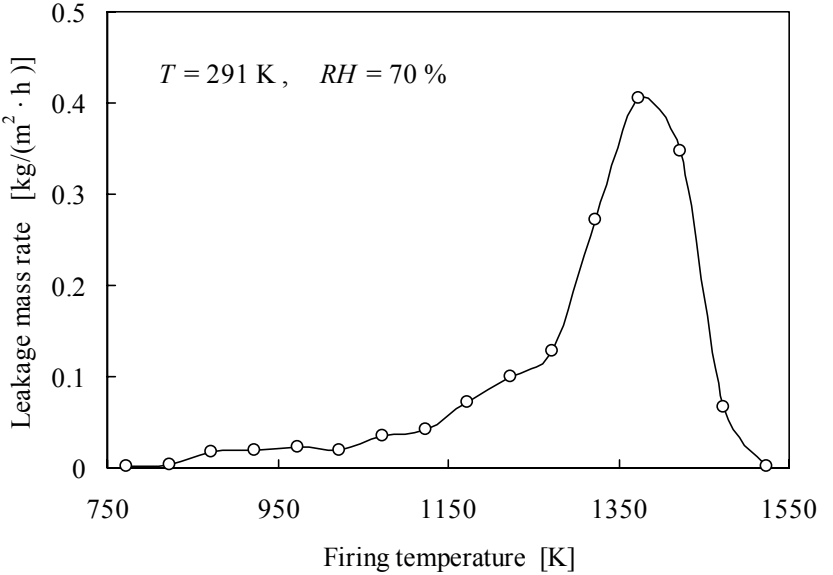

Figure 3: Effects of firing temperature on the water leakage mass rate.

3.2 Effects of the firing temperature on the evaporation rate

Figure 4 shows the effect of the firing temperature on the water evaporation rates. It is clear from the figure that the firing temperature has little effect on the water evaporation from the porous cylinders at the firing temperature of 973 ~ 1473 K. At 1523 K there was no evaporation because of no water supply to the cylinder surface. The size of the pore among the particles of semi-porcelain then affects no evaporation rate, and the nanoporous with evaporation characteristics does not consist of the pores among particles of the semi-porcelain, but of the nanoscale pores of a particle.

3.3 Effects of air temperature and humidity

Figures 5 and 6 show the effects of the temperature and relative humidity of the ambient air surrounding the cylinder. The air temperature and relative humidity must be included in the terms of non-dimensional parameters, but they still have some effects on the evaporation rates. It is not known whether this comes from the insufficient estimation of physical properties such as the diffusion coefficients, viscosity and density or fundamentally from the evaporation from the porous cylinder surface.

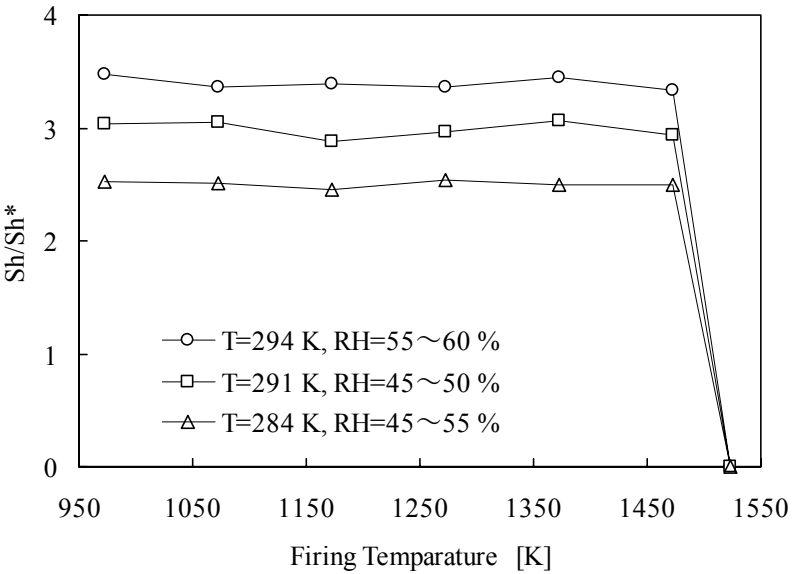

Figure 4: Effects of firing temperature on the Sherwood number ratio.

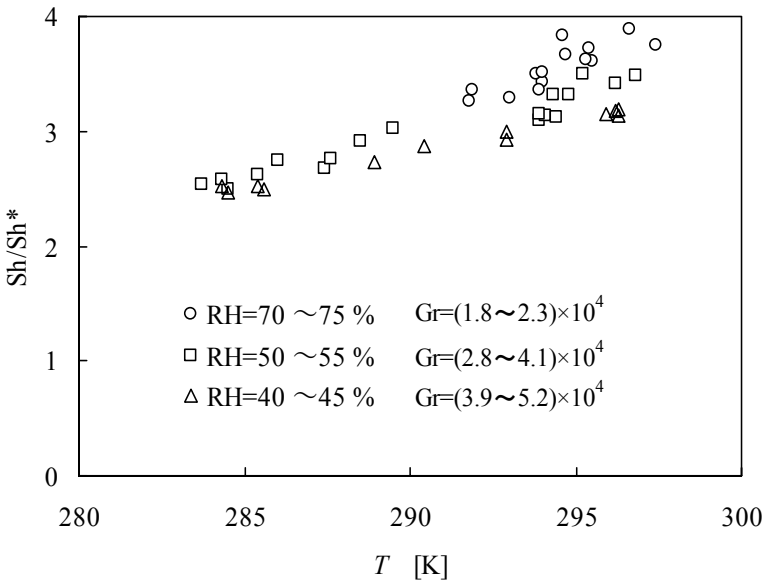

Figure 5: Effects of air temperature on the Sherwood number ratio.

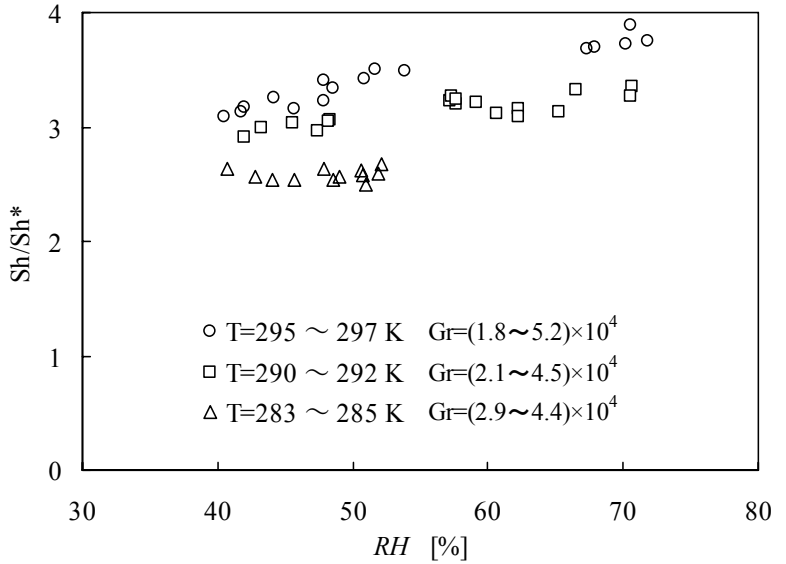

Figure 6: Effects of relative humidity on the Sherwood number ratio.

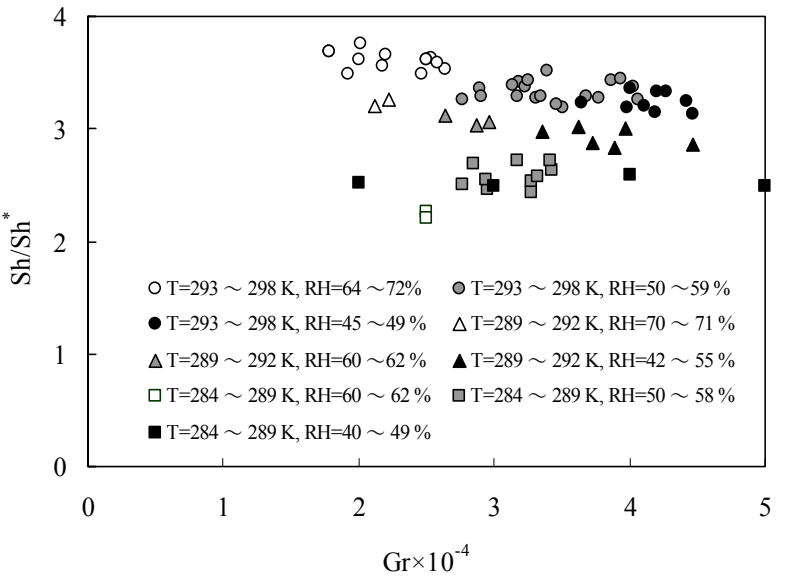

Figure 7: Effects of Grashof number on the Sherwood number ratio.

3.4 Effects of Grashof number

As shown in figure 7, the evaporation rate increases 2.5 to 4 times compared with the fully wetted cylinder surfaces in the range of the Grashof number (1~5) $\times 10^4$. In this range, the Grashof number does not show an appreciable effect on the evaporation characteristics. Specifically the macroscopic flow due to the natural convection is the same as that of the evaporation from the non-porous cylinder fully wetted by water, but those microscopic features of evaporation must be appreciably affected by the interaction of water molecules with porous material of nanoscale configuration, which gives constants 2.5 to 4 times as large as those in eqn. (13).

4 Concluding remarks

(1) Following figures 5, 6 and 7, the evaporation features depend on the ambient temperature and relative humidity, almost independent of the Grashof number. Due to this independency, the same convective flows will appear if induced by the buoyancy force by the difference of density distribution. As far as the macroscopic flows, the same flows will appear even when the evaporation mechanism itself is different from each other. If the nanoporous surface affects only the microscopic mechanism of evaporation, that is, the interaction between water and porous-surface molecules, the evaporation features must be influenced by the ambient temperature and relative humidity, independent of the Grashof number which gives the macroscopic flow field. The particular evaporation mechanism on the porous surface is not straightforwardly deducible because the molecular interaction includes the quantum effects which cannot be expected by the molecular dynamics with a constant potential of interfacial molecules.
(2) Following figure 4, the nanoporous related to the evaporation characteristics does not consist of the pores among particles of the semi-porcelain, but of the nanoscale pores of a particle of the semi porcelain.

Nomenclature

d : diameter of cylinder, m
D : diffusion coefficient, m^2/s
g : gravitational acceleration, m/s^2
Gr : Grashof number, $\mathrm{Gr} = d^3 \cdot g\left(\rho_\infty - \rho_w\right)/\left(\rho_\infty \cdot \nu^2\right)$
h_D : mass transfer rate, m/s
l : length of cylinder, m
RH : relative humidity, %
S : total surface area causing evaporation, m^2
Sh : Sherwood number, $\mathrm{Sh} = h_D \cdot d / D$.
Sh^* : Sherwood number of fully wetted surface cylinder in the handbook,

$$\mathrm{Sh}^{*} = 0.515\left(\mathrm{Gr}\cdot\mathrm{Sc}\cdot d/l\right)^{1/4} + 0.683\left(\mathrm{Gr}\cdot\mathrm{Sc}\cdot d/l\right)^{1/24}$$

Sc : Schmidt number, $\mathrm{Sc} = \nu / D$.
T : temperature, K
u : characteristic velocity, m/s
ν : kinematic viscosity, m^2/s
ρ_w : density at wall surface, kg/m^3
ρ_∞ : density of main flow, kg/m^3

References

[1] Krim, J., Coulomb, J.P. & Bouzidi, J., Triple-Point Wetting and Surface Melting of Oxygen Films Adsorbed on Graphite, *J. Phys. Review Letters* , **58 (6)**, pp. 583-586, 1987.

[2] Sokol, P.E., Ma, W.J., Herwig. K.W., Snow, W.M., Wang, Y., Koplic, J. & Banavar, J.R., Freezing in Confined Geometries, *Appl. Phys. Lett.* **61 (7)**, pp. 777-779, 1992.

[3] Molz, E., Wong, A.P.Y., Chan, M.H.W. & Beamish, J.R., Freezing and Melting of Fluids in Porous Grlasses, *Phys. Review B,* **48 (9)**, pp. 5741-5750, 1993.

[4] Unruh, K.M., Huber, T.E. & Huber, C.A., Melting & Freezing Behaviour of Indium Meta in Porous Glasses, *Phys. Review B*, **48 (12)**, pp. 9021-9027, 1993.

[5] Hansen, E.W., Stöcker, M. & Schmidt, R., Low-Temperature Phase Transition of Water Confined in Mesopores Probed by NMR. Influence on Pore Size Distribution, *J. Chem. Phys.,* **100 (6)**, pp. 2195-2200, 1996.

[6] Maddox, M.W. & Gubbins, K.E., A Molecular Simulation Study of Freezing/Melting Phenomena for Lennard-Jones Methane in Cylindrical Nanoscale Pores, *J. Chem. Phys.* **107 (22)**, pp. 9659-9667, 1997.

[7] Hara, S. & Suzuki, T., Water Evaporation on a Nanoporous Cylinder in Forced Airflows, *Thermal Science & Engineering*, **6(4),** pp. 33-38, 1998.

[8] Hara, S., Water Evaporation on a Nanoporous Cylinder in Forced Airflows, *Thermal Science & Engineering*, **8(2)**, pp. 21-27, 2000.

[9] JSME, *Heat Transfer Handbook*, Japan Society of Mechanical Engineer, pp. 144-154, 1997.